Journal of Electron Spectroscopy and Related Phenomena 185 (2012) 518–522

Contents lists available at SciVerse ScienceDirect

Journal of Electron Spectroscopy and Related Phenomena

journal homepage: www.elsevier.com/locate/elspec

The combined energy analyzer composed of electrostatic mirror fields

B.U. Ashimbaeva[a], K.Sh. Chokin[a], A.O. Saulebekov[b,*], Zh.T. Kambarova[c]

[a] Institute of Physics and Technology, Ibragimov str. 2, Almaty 480082, Kazakhstan
[b] Lomonosov Moscow State University, Kazakhstan Branch, Kajimukan str.11, Astana 010010, Kazakhstan
[c] Karaganda State University, Universitetskaya str. 28, Karaganda 100028, Kazakhstan

ARTICLE INFO

Article history:
Received 17 March 2012
Received in revised form 21 October 2012
Accepted 21 October 2012
Available online 29 October 2012

Keywords:
Cylindrical mirror
Hyperbolic mirror
Electron-optical properties
Energy resolution
Second-order focusing

ABSTRACT

A model of an electrostatic spectrometer for the energy analysis of charged particles has been calculated. The instrument is based on a combination of hyperbolic and cylindrical mirrors. The scheme for an energy- and angle-resolved spectrometer which provides angular second-order focusing, high luminosity and exit angle 90° from the source has been theoretically substantiated.

1. Introduction

Investigations of analytical properties of the combined systems, which are constructed from the various types of electrostatic mirrors, showed the possibility of expanding their functional abilities as compared to single mirrors. There are many efficient energy analyzers based on a combination of the cylindrical and spherical mirrors. The electron-optical characteristics of the energy analyzers, which are composed of successively arranged electrostatic spherical mirror (SM) and cylindrical mirror (CM) were calculated and the angular second-order focusing schemes were allocated in Ref. [1].

One of the high-luminosity electrostatic mirrors is a hyperbolic mirror (HM). Zashkvara et al. conducted a research of HM focusing schemes [2]. The hyperbolic field is nonuniform in a planar plane and has strongly distinctive dispersive properties. The study of the combined system that includes HM deserved attention and is of a practical interest. Hyperbolic field also is studied in Ref. [3], which represents the energy analyzer having an axially symmetric field structure, similar to that of a cylindrical mirror analyzer, but differing from the latter in the nonuniformity of the field strength along the symmetry axis. The difference field corresponding to the optimum configuration of an analyzer is a superposition of the hyperbolic and cylindrical fields.

In this work, the electron-optical characteristics of an electrostatic energy analyzer, which is a combination of successively arranged hyperbolic and cylindrical mirrors, are calculated. The novelty of this device is a new relative arrangement of electron mirrors in two cascade energy analyzer, which admits inject a charged particles beam in a HM field at angles that are close to a right angle with respect to the field axis.

2. Equations for description of the combined electrostatic mirrors

In this section, the electron-optical characteristics defining the motion of particles in the energy analyzer that is a combination of axially symmetric hyperbolic and cylindrical mirrors, are calculated. The scheme of the electrostatic mirror energy analyzer is shown in Fig. 1.

The analyzer consists of a point source (1) and two successively arranged mirrors with a hyperbolic (2) and cylindrical (3) distribution of fields and the detector. HM is formed by two conical electrodes (4) being under the zero potential, and a hyperbolic electrode (5) which has a potential of the same sign as the charge of the particles.

The section plane r, z of the system is shown in Fig. 1(a). Here the upper half that symmetric to the axis z is shown only for HM, and the lower half that also symmetric to the axis z is shown only for CM. Axially symmetric hyperbolic field is made by rotation conical electrodes (Fig. 1b) and hyperbolic electrode (Fig. 1c) around the axis z, and axially symmetric cylindrical field by rotation electrodes (7) and (8) around the axis z (Fig. 1d).

* Corresponding author. Tel.: +7 701 326 0325; fax: +7 717 235 3405.
E-mail address: saulebekov@mail.ru (A.O. Saulebekov).

0368-2048/$ – see front matter © 2012 Elsevier B.V. All rights reserved.
http://dx.doi.org/10.1016/j.elspec.2012.10.008

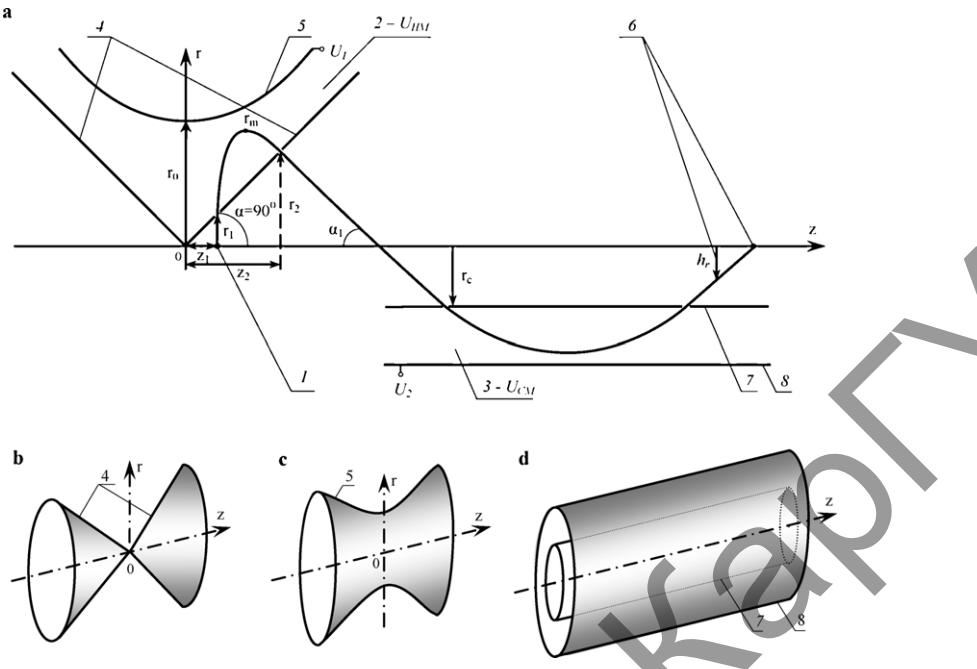

Fig. 1. The combined mirror energy analyzer scheme. (a) The energy analyzer in a section by the plane of *r*, *z*: 1 – the source of a charged particle beam, 2 – HM, 3 – CM, 4 – the transparent conical electrodes, 5 – the hyperbolic electrode, 6 – the source image, 7 – the inner cylindrical electrode, 8 – the outer cylindrical electrode. (b) The conical electrodes. (c) The hyperbolic electrode. (d) CM.

The charged particles beam comes from of a point source located on the symmetry axis z of the combined system, and enters into the region of the HM field through transparent parts of the conical electrode. The beam reflects from the hyperbolic electrode and passes again through the conical electrode and then enters to CM. A point or a ring-shape image (6) is formed at the exit of CM on the symmetry axis of the combined system.

Let us consider a motion of a charged particle in the electrostatic axially symmetric hyperbolic field that has a potential $U_{HM}(r, z)$ described in the cylindrical coordinate system r, z, φ by the following Eq. (1) [2]

$$U_{HM}(r,z) = U_1 g(r,z), \quad g(r,z) = \left(\frac{r^2}{2} - \frac{z^2}{2}\right) \tag{1}$$

According to Eq. (1), if $U_{HM} = 0$, the shape of zero-equipotential line is defined by the expression $r^2 = z^2$; therefore, the coordinates of trajectory's entrance and exit from HM can be found as $r_1^2 = z_1^2$, $r_2^2 = z_2^2$.

Let us write down equations of the charged particles motion in a HM field

$$m\ddot{r} = -qU_1\left(\frac{\partial g}{\partial r}\right) = -qU_1 r \tag{2a}$$

$$m\ddot{z} = -qU_1\left(\frac{\partial g}{\partial z}\right) = qU_1 z \tag{2b}$$

where q is an analyzed particle charge.

If the initial particle velocities are $\dot{r}_A = \upsilon_0 \sin\alpha$, $\dot{z}_A = \upsilon_0 \cos\alpha$, the integration of the system of Eqs. (2a) and (2b) gives the next differential equation of the particles motion:

$$\pm\frac{dr}{\sqrt{S^2 - r^2 + r_1^2}} = \frac{dz}{\sqrt{S^2\cot^2\alpha + z^2 - z_1^2}} \tag{3}$$

where $S = \sqrt{2(W/qU_1)}\sin\alpha$ is the reflection parameter of HM that connects mirror's geometry and energy characteristics. The parameter W corresponds to the particle kinetic energy. The sign (+) in Eq. (3) corresponds to the rising section of the trajectory, and the sign (−) – to the declining section of the trajectory in HM field. All parameters with length dimension are expressed in units of central radius r_0 of HM deflecting electrode (Fig. 1).

After integration of differential Eq. (3) within the limits from r_1 to the trajectory vertex r_m at the rising section of the trajectory and from r_m to r_2 at the declining section of the trajectory, the equation connecting the entrance point z_1 and the exit point z_2 of trajectory from the HM is found

$$\pi - \arcsin\frac{z_1}{\sqrt{S^2 + z_1^2}} - \arcsin\frac{z_2}{\sqrt{S_1^2 + z_2^2}} = \ln(z_2 + S_1\cot\alpha_1) - \ln(z_1 + S\cot\alpha) \tag{4}$$

where $S_1 = S(\sin\alpha_1/\sin\alpha)$.

The trajectory exit angle α_1 from HM field is determined from Eq. (3) on condition $r^2 = r_2^2$ and $z^2 = z_2^2$

$$\cot\alpha_1 = \sqrt{\frac{S^2\cot^2\alpha + z_2^2 - z_1^2}{S^2 - z_2^2 + z_1^2}}. \tag{5}$$

The radial coordinate of a trajectory turning point r_m in HM field is calculated from Eq. (3), at the condition $(dr/dz) = 0$

$$S^2 - r_m^2 + r_1^2 = 0, \quad r_m^2 = S^2 + r_1^2 \tag{6}$$

The equation of radial coordinates of both trajectory branches at the turning point $r_m = r_m^{(1)} = r_m^{(2)}$ gives an additional formula to calculate the right trajectory branch in the HM field z_2, S_1

$$z_2^2 + S_1^2 = z_1^2 + S^2. \tag{7}$$

To study characteristics of combined mirror system, it is necessary to determine an expression for a projection of the planar trajectory onto the symmetry axis z from the source to its image as a function of mirrors system parameters. According to Fig. 1, this quantity is the sum of trajectory projections in HM and CM. The trajectory projection parameters in HM are calculated from Eqs. (4)–(7). The solution of transcendental Eq. (4) is determined by the successive approximate method when the quantities S, z_1, z_2 are varied. The trajectory projection in electrostatic CM is calculated in

accordance to the results in [4]. The total projection for HM and CM system l is given by the relations

$$l = l_{HM} + l_{CM}, \quad l_{HM} = z_2(1 + \cot\alpha_1) - z_1,$$

$$l_{CM} = \frac{l_{CM}}{r_0} = \mu \cot\alpha_1(2 + 4P_1\theta_1 - h_r). \tag{8}$$

Here $P_1^2 = (W/qU_2)\sin^2\alpha_1$, $\theta_1 = e^{P_1^2}\int_0^{P_1} e^{-x_1^2}$ are the reflection parameters of CM, h_r is a quantity defining the distance of an image from the analyzer's z axis, $\mu = (r_c/r_0)$ is a coefficient that determines the quantity of inner cylindrical electrode radius r_c in units of r_0. The radius of the trajectory vertex in the CM field is calculated from equation $r_m = \mu \exp(P_1^2)$.

3. Calculation of electron-optical characteristics of the combined system of electrostatic mirrors

The current section includes a calculation of aberrations that determines conditions of a charged particles beam focusing in the proposed combined mirrors system. If a particles beam enters an analyzer with the angular spread $\pm\Delta\alpha$ in an axial plane and the energy spread $\Delta\varepsilon = (W - W_0)/W_0$ (where W_0 is the ground value of the particle kinetic energy), the quantity of the total projection l can be decomposed into the Taylor series, providing $\Delta\alpha$ and $\Delta\varepsilon$ as the small perturbations [4]

$$l = l_0 + \frac{\partial l}{\partial\alpha}\Delta\alpha + \frac{\partial l}{\partial\varepsilon}\Delta\varepsilon + \frac{1}{2!}\frac{\partial^2 l}{\partial\alpha^2}(\Delta\alpha)^2 + \dots \tag{9}$$

An angular first-order focusing is fulfilled at $(\partial l/\partial\alpha) = 0$; and the angular second-order focusing – at $(\partial l/\partial\alpha) = (\partial^2 l/\partial\alpha^2) = 0$. The quantity of $\Delta l = (\partial l/\partial\varepsilon)\Delta\varepsilon$, from Eq. (9) characterizes the dispersive properties and determines the value of image displacement when a particles beam energy changes.

The following equations determine a first-order aberration $(\partial l/\partial\alpha)$ and a dispersion $(dl/d\varepsilon)$ coefficients of the combined mirror system:

$$\frac{dl}{d\alpha} = (1 + \cot\alpha_1)\frac{dz_2}{d\alpha} + f\frac{d\alpha_1}{d\alpha} \tag{10}$$

where

$$(1 + \cot\alpha_1)\frac{dz_2}{d\alpha} = S\cot\alpha\cot\alpha_1\frac{z_1S_1 + z_2S}{z_1^2 + S^2} + \frac{S^2\cot\alpha}{b_1} - \frac{SS_1\cot\alpha_1}{b}, \tag{11}$$

$$f = 4\mu\omega\cot^2\alpha_1 - (1 + \cot^2\alpha_1)[z_2 + \mu(2 + 4P_1\theta_1 - h_r)], \tag{12}$$

$$\frac{d\alpha_1}{d\alpha} = \frac{S^2\cot\alpha_1 - z_2(dz_2/d\alpha)}{S_1^2\cot\alpha_1}, \tag{13}$$

$$\omega = P_1\theta_1 + P_1^2(1 + 2P_1\theta_1), \quad b = z_1 + S\cot\alpha, \quad b_1 = z_2 + S_1\cot\alpha_1, \tag{14}$$

and

$$\frac{dl}{d\varepsilon} = (1 + \cot\alpha_1)\frac{dz_2}{d\varepsilon} + 2\mu\omega\cot\alpha_1 + f\frac{d\alpha_1}{d\varepsilon}, \tag{15}$$

where

$$(1 + \cot\alpha_1)\frac{dz_2}{d\varepsilon} = \frac{1}{2}\left[S\cot\alpha_1\frac{z_1S_1 + z_2S}{z_1^2 + S^2} - \frac{S^2}{b_1}\cot^2\alpha - \frac{SS_1}{b}\cot\alpha\cot\alpha_1\right], \tag{16}$$

$$\frac{d\alpha_1}{d\varepsilon} = \frac{S^2 - S_1^2}{2S_1^2\cot\alpha_1} - \frac{z_2}{S_1^2\cot\alpha_1}\frac{dz_2}{d\varepsilon}. \tag{17}$$

The second-order aberration coefficient is determined by the following equations

$$\frac{d^2 l}{d\alpha^2} = (1 + \cot\alpha_1)\frac{d^2 z_2}{d\alpha^2} - (1 + \cot^2\alpha_1)\frac{dz_2}{d\alpha}\frac{d\alpha_1}{d\alpha} + \frac{df}{d\alpha}\frac{d\alpha_1}{d\alpha} + f\frac{d^2\alpha_1}{d\alpha^2}, \tag{18}$$

where

$$(1 + \cot\alpha_1)\frac{d^2 z_2}{d\alpha^2} = (1 + \cot^2\alpha_1)\frac{d\alpha_1}{d\alpha}\frac{dz_2}{da} + f_1 + f_2 + f_3, \tag{19}$$

$$\frac{df}{d\alpha} = 4\mu\frac{d\omega}{d\alpha}\cot^2\alpha - (1 + \cot^2\alpha_1)\frac{dz_2}{d\alpha} + \cot\alpha_1(1 + \cot^2\alpha_1)\frac{d\alpha_1}{d\alpha} \times [2z_2 + \mu(4 + 8P_1\theta_1 - 2h_r) - 12\mu\omega], \tag{20}$$

$$\frac{d^2\alpha_1}{d\alpha^2} = \frac{1}{S_1^2\cot\alpha_1}\left[S^2(\cot^2\alpha - 1) - \left(\frac{dz_2}{d\alpha}\right)^2 - z_2\frac{d^2 z_2}{d\alpha^2}\right] + \frac{(1 - \cot^2\alpha)}{\cot\alpha_1}\left(\frac{d\alpha_1}{d\alpha}\right)^2 \tag{21}$$

$$\frac{d\omega}{d\alpha} = \left[\omega(1 + 2P_1^2) + 2P_1^2(1 + 2P_1\theta_1)\right]\frac{d\alpha_1}{d\alpha}\cot\alpha_1 \tag{22}$$

$$f_1 = -S\cot\alpha_1\frac{z_1S_1 + z_2S}{z_1^2 + S^2} \times \left[1 + \frac{\cot\alpha(1 + \cot\alpha_1)}{\cot\alpha_1}\frac{d\alpha_1}{d\alpha} + 2\frac{S^2\cot^2\alpha}{z_1^2 + S^2}\right] + \frac{S\cot\alpha_1}{z_1^2 + S^2}\left[z_1S_1\cot\alpha\frac{d\alpha_1}{d\alpha} + S\frac{dz_2}{d\alpha} + z_2S\cot\alpha\right] \tag{23}$$

$$f_2 = \frac{S^2}{b_1}(\cot\alpha - 1) - \frac{S^2\cot\alpha_1}{b_1^2}\left(\frac{dz_2}{d\alpha} - S_1\frac{d\alpha_1}{d\alpha}\right) \tag{24}$$

$$f_3 = -\frac{SS_1\cot\alpha_1}{b}\left(\cot\alpha + \frac{S}{b}\right) + \frac{SS_1}{b} \tag{25}$$

For the analysis of the focusing and dispersion properties of the combined system by Eqs. (10)–(25), the electron-optical parameters which satisfied the angular second-order focusing $\frac{dl}{d\alpha}\Big|_{\alpha=90^\circ} = \frac{d^2 l}{d\alpha^2}\Big|_{\alpha=90^\circ} = 0$ have been calculated. The results of calculation are presented in Table 1, that includes the following quantities: $\mu = (r_c/r_0)$ and z_1, z_2 (Fig. 1), S, S_1 – the reflection parameter of HM, r_m (HM) and r_m (CM) – the radii of the turning points of the trajectory, P_1 – the reflection parameter of CM, α_1 – the trajectory exit angle from HM field, h_r – the quantity showing the distance between the image and the symmetry axis of the combined mirrors system, $D = (\partial l/\partial\varepsilon)$ – the relative linear dispersion in energy, $l = l/r_0$ – the total projection of a trajectory onto the symmetry axis of mirrors from a source to its image corresponding to the angular second-order focusing regime.

Analysis of the data in Table 1 shows that in the analyzer combined of cylindrical and hyperbolic mirrors, the angular second-order focusing is achieved over a wide range of μ, S, z_1, z_2 parameters for the schemes with $0 \prec h_r \prec 1$. The schemes of analyzers with $h_r \succ 1$ have no practical meaning, since the source image is located in the CM field. On the contrary, the schemes with $0 \prec h_r \prec 1$ can be practically implementable. In Table 1, there are parameters of two analyzers with the value of $h_r = 0$. These parameters characterize the charged particles beam that (emitted from a

Table 1
The electron-optical characteristics of angular second-order focusing schemes of the combined mirror system.

No.	z_2	S	S_1	r_m (HM)	r_m (CM)	P_1	α_1	h_r	D	l
$\alpha = 90^\circ$, $z_1 = 0.2$, $\mu = 0.7$										
1	0.8320	1.0840	0.7231	1.1023	1.3371	0.7982	41.8390	1.6575	5.62	4.96
2	0.8410	1.1040	0.7427	1.1220	1.3758	0.8159	42.2753	1.5325	5.91	5.22
3	0.8530	1.1310	0.7691	1.1485	1.4307	0.8395	42.8467	1.3478	5.32	5.58
4	0.8630	1.1540	0.7918	1.1712	1.4805	0.8596	43.3249	1.1717	6.70	5.91
5	0.8910	1.2200	0.8570	1.2363	1.6371	0.9162	44.6273	0.5720	7.93	6.95
6	0.8920	1.2225	0.8596	1.2388	1.6439	0.9185	44.6775	0.5444	7.99	7.00
7	0.8926	1.2239	0.8609	1.2401	1.6473	0.9196	44.7028	0.5307	8.01	7.02
8	0.8930	1.2249	0.8619	1.2411	1.6500	0.9205	44.7228	0.5196	8.04	7.04
9	0.9000	1.2420	0.8790	1.2580	1.6953	0.9351	45.0476	0.3321	8.41	7.34
10	0.9101	1.2668	0.9036	1.2824	1.7635	0.9560	45.5038	0.0414	8.97	7.80
11	**0.9114**	**1.2700**	**0.9068**	**1.2856**	**1.7727**	**0.9587**	**45.5630**	**0.0009**	**9.05**	**7.86**
12	0.9123	1.2723	0.9091	1.2879	1.7793	0.9606	45.6047	−0.0279	9.10	7.91
13	0.9182	1.2871	0.9239	1.3026	1.8226	0.9731	45.8724	−0.2203	9.47	8.20
$\alpha = 90^\circ$, $z_1 = 0.2$, $\mu = 1$										
1	0.8320	1.0840	0.7231	1.1023	1.8542	0.7858	41.8390	1.2110	6.94	6.67
2	0.8410	1.1040	0.7427	1.1220	1.9090	0.8041	42.2753	1.0754	7.37	7.04
3	0.8530	1.1310	0.7691	1.1485	1.9866	0.8285	42.8467	0.8760	7.98	7.56
4	0.8630	1.1540	0.7918	1.1712	2.0571	0.8493	43.3249	0.6872	8.55	8.03
5	0.8910	1.2200	0.8570	1.2363	2.2789	0.9076	44.6273	0.0507	10.39	9.52
6	0.8920	1.2225	0.8596	1.2388	2.2884	0.9099	44.6775	0.0217	10.47	9.58
7	0.8926	1.2239	0.8609	1.2401	2.2933	0.9110	44.7028	0.0072	10.52	9.61
8	**0.8929**	**1.2246**	**0.8616**	**1.2408**	**2.2957**	**0.9116**	**44.7151**	**−0.0001**	**10.54**	**9.63**
9	0.8930	1.2249	0.8619	1.2411	2.2971	0.9119	44.7228	−0.0046	10.55	9.64
10	0.9000	1.2420	0.8790	1.2580	2.3614	0.9269	45.0476	−0.2018	11.10	10.07

point source) focuses to a point on the symmetry axis of the analyzer. The parameters of «axis-axis» focusing are marked by bold font in Table 1. The scheme of the combined mirror system that is shown in Fig. 1 corresponds to the parameters: $\alpha = 90^\circ$, $z_1 = 0.2$, $z_2 = 0.9114$, $S = 1.2700$, $S_1 = 0.9068$, $P_1 = 0.9587$.

A characteristic feature of the energy analyzer based on described mirrors system is realization of the second-order angular focusing for many electron-optical systems. The possibility to vary the free parameters μ, S, z_1, z_2 enables one to design various schemes of the angular focusing. Some of these parameters are presented in Table 1. This quality of the combined analyzer is of interest because it leads to the expansion of the analytical capabilities of this device.

4. Possibility of energy- and angle-analysis in the system of HM and CM

The scheme for an energy- and angle-resolved spectrograph which provides high-quality angular focusing of charged particles beams of various energies along the focal surface shaped as a right circular cone was presented in Ref. [5]. An energy analyzer has been composed of successively arranged electrostatic spherical mirror and the cascades of internal and external reflection of a charged particles beam in the CM. In such case simultaneous registration of the finite intervals of charged particle distribution in both energy and angle by means of a position-sensitive detector of a relatively simple conic form, repeating a focal surface, is possible in practice.

The angular spectra allow obtaining additional information about an investigated object, for example, about the band structure of surface layers.

Express energy- and angle-analysis of the photoelectrons is possible only by means of high-luminosity energy analyzers. This requirement is met by a few known devices, including ESA-22 electrostatic electron spectrometer [6]. The spectrometer consists of SM and CM. In this paper the energy- and angle-resolved electrostatic spectrometer on the basis of the HM and CM is proposed, i.e. HM is used in place of SM. The energy- and angle-resolved electrostatic spectrometer scheme on basis of the HM and CM is shown in Fig. 2.

A distinctive quality of the proposed mirror analyzer is the property to analyze charged particles beams emitted by the source at angles close to a right angle (90°). This focusing angle allows building an effective diagram of angular measurements [7], and the second-order focusing means realization of the requirement of high luminosity and resolution's combination.

According to the scheme (Fig. 2), a point source S, placed at the symmetry axis, injects the fan-shaped charged particles beam ($\varphi \leq 90^\circ$) into the spectrometer with the mid-plane being perpendicular to the symmetry axis z, the beam's opening angle in the mid-plane is 180°. The HM forms an intermediate ring-shape image J' of the source S which, in turn, is transformed into the point image J situated at the symmetry axis in the second cascade of reflection — in CM. The spectrometer has a reception diaphragm (4) with a circular slit centered at the point J. In the analytical methods at using of energy analyzers with well-focused beams of primary radiation an emitter is considered to be a point. This approximation is sufficient for the primary particles beams with a cross-sectional diameter of 10 μm or less and the inner cylindrical electrode of 50 mm in diameter.

In the work, the analyzer resolution was calculated for the optimum size of the reception diaphragm for the case of a point emitter. In such optimal case, the reception diaphragm of corresponding width is located in the place of the smallest cross-section of the detected particles beams. The optimality follows from the fact, that at decreasing of the diaphragm's width, the luminosity (input solid angle) decreases also, while at increasing of the diaphragm's width, the luminosity does not increase, and the resolution worsens and the vertex of the instrument function of the analyzer becomes planar and not sharp as it is in the optimal case. Note that it makes sense to compare the different analyzers in the mode of optimal operation.

In any energy spectrum interval resolved by a dispersion CM the initial charged particle distribution in angles φ can be registered simultaneously by means of a position-sensitive detector (5) placed behind diaphragm (4). The advantage is the high energy resolution achieved due to angular second-order focusing of this mirror system.

The relative energy resolution of the combined analyzer is $\Delta E/E = 0.28\%$ at an entrance divergence angle 4°, the luminosity is

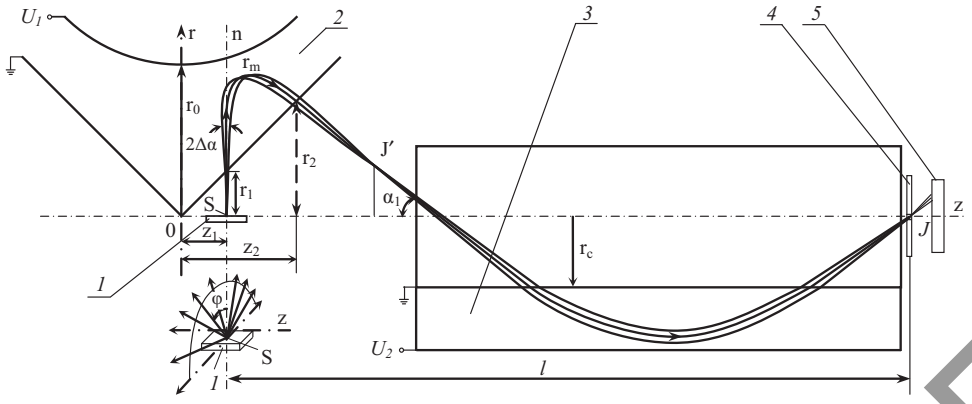

Fig. 2. The energy- and angle- resolved spectrometer scheme. *S* – the source of a charged particles beam, *J* – the source image, *J′* – the intermediate focus, 1 – the specimen with point source, 2 – HM, 3 – CM, 4 – the reception diaphragm with a central opening, 5 – the position-sensitive detector.

Table 2
Comparison of the parameters of various electrostatic analyzers: the classical CMA [9], the distorted field CMA [10], the distorted field CMA with conical ends (CMACE) [8], the ESA-21 triple-pass electron spectrometer [11] and the case concerned the present calculations. All calculated values are related to the second-order focusing.

Number of version	α_0	l	n	D_r
[9]	42.3°	6.129	0.529	0.914
[10]	43.5°	5.707	0.581	1.202
[8]	90°	11.59	0.905	1.505
[11]	90°	17.016	0.590	0.983
Present work	90°	7.86	1.24	1.15

3.5% of 2π. The energy resolution of a combined energy analyzer is increasing with decreasing the divergence angle of the entering beam and close by 2° it may be better than 0.08%.

Let us continue the comparison of the parameters of analyzers, which was begun in [8]. The calculated parameters and focusing properties of the analyzer are shown in Table 2, and are compared with the parameters of the analyzers, which previously have been calculated.

The relative energy dispersion is defined by [8]

$$D_r(\alpha = \alpha_0) = -\frac{\Delta l}{l}\frac{n}{\Delta n(1\%)}$$

where $n = qU_1/W_0$ is the spectrometer constant, $\Delta n(1\%)$ corresponds to the change in n for 1% relative change in the energy of the electrons passing through the analyzer.

For the entrance angle 90° the analyzer proposed in this paper has the shortest length, however it is not worse in the dispersion, as it can be seen in Table 2.

5. Conclusions

The equation for the total projection of a charged particle trajectory in the combined system of successively arranged hyperbolic and cylindrical electrostatic mirrors was derived. The aberration coefficients and many different schemes of angular second-order focusing in the axial plane of the analyzer were calculated. The electron-optical characteristics for these schemes were analyzed.

The electron-optical parameters of the optimal scheme of the combined energy analyzer were determined. The scheme is able to operate in high resolution and high luminosity regime. This combination, together with the ability to analyze charged particles beams emitted from the source at angles close to 90°, allows using this scheme as an energy- and angle-resolved spectrometer.

The proposed electron-optical system can be applied in the double spectrograph regime taking both the energy and angular spectra.

References

[1] V.V. Zashkvara, A.O. Saulebekov, L.S. Yurchak, A.I. Chasnikov, Sov. Phys. – Tech. Phys. (English Transl.) 37 (6) (1992) 663.
[2] V.V. Zashkvara, A.M. Il'in, V.F. Kruchkov, Zh. Tekh. Phys. 46 (1976) 1572 (in Russian).
[3] K. Siegbahn, N. Kholine, G. Golikov, Nuclear Instrum. Methods A 384 (1997) 563.
[4] V.V. Zashkvara, M.I. Korsunski, O.S. Kosmachev, Sov. Phys. – Tech. Phys. (English Transl.) 11 (1966) 96.
[5] V.V. Zashkvara, B.U. Ashimbaeva, Nuclear Instrum. Methods A 340 (1994) 514.
[6] S. Ricz, Á. Kövér, M. Jurvansuu, D. Varga, J. Molnár, S. Aksela, Phys. Rev. A 65 (2002) 042707.
[7] A. Kover, D. Varga, Gy Szabo, D. Berenyi, I. Kadar, J. Vegh, G. Hock, J. Phys. B 16 (1983) 1017.
[8] D. Varga, K. Tőkési, I. Rajta, J. Electron Spectrosc. Relat. Phenom. 76 (1995) 433.
[9] J.S. Risley, Rev. Sci. Instrum. 43 (1972) 95.
[10] D. Varga, Á. Kádár, L. Kövér, L. Redler, Nuclear Instrum. Methods A 238 (1985) 393.
[11] D. Varga, I. Kádár, S. Ricz, J. Végh, Á. Kövér, B. Sulik, D. Berényi, Nuclear Instrum. Methods A 313 (1992) 163.